

## Heteroleptic iron(II) complexes with naphthoquinone-type ligands

 Takuya Shiga,<sup>\*a</sup> Rina Kumamaru,<sup>a</sup> Graham N. Newton<sup>b</sup> and Hiroki Oshio<sup>a,c</sup>

 Received 00th January 20xx,  
 Accepted 00th January 20xx

DOI: 10.1039/x0xx00000x

www.rsc.org/

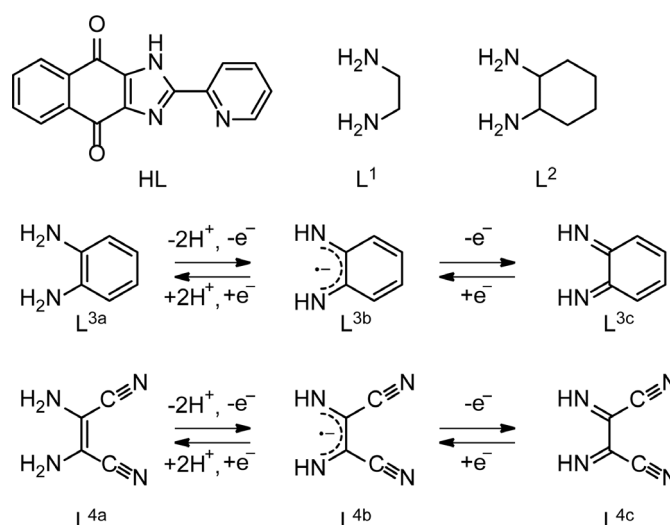
Heteroleptic iron complexes with a naphthoquinone-type ligand, 2-(pyridin-2-yl)-1*H*-naphtho[2,3-*d*]imidazole-4,9-dione (HL), were synthesized, and their structures and magnetic properties were investigated. Two spin-crossover complexes, [Fe(L)<sub>2</sub>(L<sup>1</sup>)] (**1**, L<sup>1</sup> = ethylenediamine) and [Fe(L)<sub>2</sub>(L<sup>2</sup>)] (**2**, L<sup>2</sup> = cyclohexanediamine) were structurally characterized at 100 K and 270 K, and their gradual spin crossover behavior observed by magnetic susceptibility measurements and confirmed by Mössbauer spectroscopic analyses. Two homologous iron(II) complexes, [Fe(L)<sub>2</sub>(L<sup>3c</sup>)] (**3**, L<sup>3c</sup> = diimino benzoquinone) and [Fe(L)<sub>2</sub>(L<sup>4c</sup>)] (**4**, L<sup>4c</sup> = iminosuccinonitrile), were found to exist in the low-spin state in the range of 10–300 K. In contrast, the corresponding complex with two water ligands, [Fe(L)<sub>2</sub>(H<sub>2</sub>O)<sub>2</sub>] (**5**), and the tris-chelate complex with protonated ligands (HL), [Fe(HL)<sub>3</sub>](BF<sub>4</sub>)<sub>2</sub> (**6**), were found to be high-spin.

### Introduction

The design and controlled fabrication of heteroleptic complexes is an important step in the development of functional molecular materials. One of the merits of heteroleptic complexes is the vast number of accessible combinations of ligands, leading to complexes with highly tuneable electronic structures and physical properties obtained through relatively simple ligand replacement or structural modifications.<sup>1</sup> Additionally, the combination of multiple ligands in a single metal complex can lead to the formation of systems with complementary ligand-derived properties. For example, the combination of electron donor and acceptor ligands can facilitate directional electron transfers in a single molecule, and such dyad and triad systems are intensively studied in the field of artificial photosynthesis.<sup>2</sup>

The electronic states of coordination compounds can be finely tuned by modifying the ligand field strength. Spin crossover (SCO) complexes are well-known switchable molecules that show reversible changes of their electronic state upon exposure to external stimuli, such as temperature, light, pressure, and guest molecules.<sup>3</sup> For iron(II) complexes, N<sub>6</sub> coordination environments can lead to SCO properties. Classical iron complexes with typical bidentate ligands with two nitrogen donors, such as [Fe(bpy)<sub>3</sub>]X<sub>2</sub> (bpy = 2,2'-

bipyridine), [Fe(phen)<sub>3</sub>]X<sub>2</sub> (phen = 1,10-phenanthroline, X is counter anion) and [Fe(en)<sub>3</sub>]X<sub>2</sub> (en = ethylenediamine), are examples of homoleptic tris-chelates,<sup>4</sup> but reports of SCO activity in such systems are limited, with a few famous exceptions, such as [Fe(pica)<sub>3</sub>]X<sub>2</sub> (pica = 2-picolylamine), [Fe(R-bik)<sub>3</sub>](BF<sub>4</sub>)<sub>2</sub> (R-bik = bis(1-*R*-imidazol-2-yl)ketone), and [Fe(py-Biim)<sub>3</sub>]X<sub>2</sub> (py-Biim = 2-(2'-pyridyl)benzimidazole).<sup>5</sup> M. Shatruk et al. discussed the spin state of homoleptic Fe(II) tris-diimine complexes based on structural metrics.<sup>6</sup> The authors concluded that the N-N distance between the chelating N-donor sites in the free ligand is important for achievement of spin crossover behavior. Heteroleptic [Fe(L<sup>A</sup>)<sub>2</sub>(L<sup>B</sup>)] (L<sup>A</sup> and L<sup>B</sup> are different bidentate ligand) SCO complexes are also known,<sup>7</sup> with [Fe(bpz)<sub>2</sub>(bpy)] and [Fe(bpz)<sub>2</sub>(phen)] (bpz = dihydrobis(pyrazolyl)borate anion) primary examples. The SCO properties of the systems were found to depend on the nature of the chosen bidentate ligands.<sup>8</sup>

Scheme 1. Naphthoquinone ligand HL and capping ligands L<sup>1</sup>, L<sup>2</sup>, L<sup>3a-c</sup>, and L<sup>4a-c</sup>.

<sup>a</sup> Graduate School of Pure and Applied Sciences, University of Tsukuba, Tennodai 1-1-1, Tsukuba, Ibaraki 305-8571, Japan.

<sup>b</sup> GSK Carbon Neutral Laboratories for Sustainable Chemistry, The University of Nottingham, Nottingham NG7 2GA, U.K.

<sup>c</sup> Prof. Dr. H. Oshio

State Key Laboratory of Fine Chemicals, Dalian University of Technology  
 2 Linggong Rd., 116024 Dalian, China

Electronic Supplementary Information (ESI) available: [packing structures of **1** and **2**, analyses of magnetic data, Mössbauer spectra, and crystal parameters]. CCDC 1956636–1956643 for **1**–**6**, respectively. For ESI and crystallographic data in CIF or other electronic format. See DOI: 10.1039/x0xx00000x

Similarly, the use of anionic monodentate ligands in heteroleptic complexes can be an effective strategy to isolate neutral complexes of bis-chelated divalent iron, with  $[\text{Fe}(\text{bpy})_2(\text{NCS})_2]$  and  $[\text{Fe}(\text{phen})_2(\text{NCS})_2]$  perhaps the most prominent examples.<sup>9</sup> Subsequent exchange of the anionic monodentate ligands allows fine control over the SCO behaviour of the system. Recently, we reported a range of functional mononuclear and polynuclear supramolecular spin crossover compounds towards the preparation of responsive systems for switchable molecular materials.<sup>10</sup> Here we present our recent findings on the synthesis and switchable properties of heteroleptic iron(II) complexes with naphthoquinone-type ligands, HL (2-(pyridin-2-yl)-1*H*-naphtho[2,3-*d*]imidazole-4,9-dione), and a range of capping ligands (Scheme 1). The naphthoquinone-type bidentate ligand HL was selected due to its monoanionic bidentate nature and was expected to provide an adequate ligand field for the Fe(II) ion. Four bidentate ligands were chosen as secondary capping ligands; ethylenediamine ( $\text{L}^1$ ), *cis*-1,2-cyclohexanediamine ( $\text{L}^2$ ), *o*-phenylenediamine ( $\text{L}^{3a}$ ) and diaminomaleonitrile ( $\text{L}^{4a}$ ).  $\text{L}^{3a}$  and  $\text{L}^{4a}$  are redox-active ligands and exhibit two-step deprotonation-dependent oxidation (Scheme 1), yielding  $\text{L}^{3b}$  ( $\text{L}^{4b}$ ) and  $\text{L}^{3c}$  ( $\text{L}^{4c}$ ). In this paper, the syntheses and electronic states of four heteroleptic mononuclear iron(II) complexes with  $\text{N}_6$  coordination environments, arising from two HL groups and one secondary capping ligand, were investigated. In addition, the syntheses and physical properties of two related complexes, one the aqua complex and the other a homoleptic tris-naphthoquinone complex, were investigated for comparison.

## Experimental

### Materials

All reagents were commercially purchased and used without further purification. All solvents were used without degassing treatment or distillation. The naphthoquinone-type ligand 2-(pyridin-2-yl)-1*H*-naphtho[2,3-*d*]imidazole-4,9-dione (HL) was synthesized according to the procedure described in reference 11.<sup>11</sup>

### Synthesis of $[\text{Fe}(\text{L})_2(\text{L}^1)]$ (1)

To a DMF solution (2 mL) of  $\text{Fe}(\text{BF}_4)_2 \cdot 6\text{H}_2\text{O}$  (15.9 mg, 0.0471 mmol) a DMF solution (6 mL) of HL (25.2 mg, 0.0915 mmol) and triethylamine (14  $\mu\text{L}$ , 0.1 mmol) was added, affording a dark green solution. Ethylenediamine ( $\text{L}^1$ , 1 mL, 15 mmol) was then added and the mixture stirred for 20 minutes. Filtration followed by diffusion of 1,4-dioxane yielded dark green plates of  $[\text{Fe}(\text{L})_2(\text{L}^1)] \cdot \text{DMF} \cdot 2(1,4\text{-dioxane})$  ( $\mathbf{1} \cdot \text{DMF} \cdot 2(1,4\text{-dioxane})$ ). The crystals were collected by suction and air-dried. Anal. Calc. for  $[\text{Fe}(\text{L})_2(\text{L}^1)] \cdot \text{H}_2\text{O} \cdot 0.5\text{DMF}$  ( $\mathbf{1} \cdot \text{H}_2\text{O} \cdot 0.5\text{DMF}$ ): C, 58.38; H, 4.64; N, 16.80 %. Found: C, 58.28; H, 4.39; N, 16.98 %. Selected IR (KBr): 1653(s,  $\nu_{\text{C=O}}$ ), 1587(m), 1465(m), 1220(s), 986(m), 708(s)  $\text{cm}^{-1}$ .

### Synthesis of $[\text{Fe}(\text{L})_2(\text{L}^2)]$ (2)

A similar synthetic method to that of **1**, except for the use of *cis*-1,2-cyclohexanediamine ( $\text{L}^2$ , 0.7 mL, 5.9 mmol) instead of

ethylenediamine. Diffusion of diisopropyl ether at 40 °C afforded  $[\text{Fe}(\text{L})_2(\text{L}^2)] \cdot \text{DMF}$  as dark green needle crystals. The crystals were collected by suction and air-dried. Anal. Calc. for  $[\text{Fe}(\text{L})_2(\text{L}^2)] \cdot \text{DMF}$ : C, 62.21; H, 4.71; N, 15.92 %. Found: C, 62.12; H, 5.12; N, 15.60 %. Selected IR (KBr): 3308(m), 2930(m), 1670(s,  $\nu_{\text{C=O}}$ ), 1651(s), 1591(s), 1466(s), 1221(s), 934(s), 710(s)  $\text{cm}^{-1}$ .

### Synthesis of $[\text{Fe}(\text{L})_2(\text{L}^{3c})]$ (3)

A similar synthetic method to that of **1**, except for the use of *o*-phenylenediamine ( $\text{L}^{3a}$ , 5.2 mg, 0.048 mmol) instead of ethylenediamine. Diffusion of tert-butylmethyl ether afforded  $[\text{Fe}(\text{L})_2(\text{L}^{3c})] \cdot 2\text{DMF}$  as dark green blocks. The crystals were collected by suction and air-dried. Anal. Calc. for  $[\text{Fe}(\text{L})_2(\text{L}^{3c})] \cdot 2\text{DMF}$ : C, 61.69; H, 4.24; N, 16.35 %. Found: C, 61.45; H, 4.31; N, 16.33 %. Selected IR (KBr): 1659(s,  $\nu_{\text{C=O}}$ ), 1466(m), 1379(m), 1223(s), 966(m), 708(m)  $\text{cm}^{-1}$ .

### Synthesis of $[\text{Fe}(\text{L})_2(\text{L}^{4c})]$ (4)

A similar synthetic method to that of **1**, except for the use of diaminomaleonitrile ( $\text{L}^{4a}$ , 28.9 mg, 0.105 mmol) instead of ethylenediamine. Diffusion of diisopropyl ether at 40 °C afforded  $[\text{Fe}(\text{L})_2(\text{L}^{4c})] \cdot 2\text{DMF}$  as dark green blocks. The crystals were collected by suction and air-dried. Anal. Calc. for  $[\text{Fe}(\text{L})_2(\text{L}^{4c})] \cdot 0.5\text{H}_2\text{O} \cdot 0.5\text{DMF}$ : C, 59.58; H, 3.00; N, 19.45 %. Found: C, 59.65; H, 3.08; N, 19.35 %. Selected IR (KBr): 2232(m, CN), 1653(s,  $\nu_{\text{C=O}}$ ), 1468(s), 1223(s), 966(m), 708(m)  $\text{cm}^{-1}$ .

### Synthesis of $[\text{Fe}(\text{L})_2(\text{H}_2\text{O})_2]$ (5)

To a DMF solution (2 mL) of  $\text{Fe}(\text{BF}_4)_2 \cdot 6\text{H}_2\text{O}$  (17.9 mg, 0.0530 mmol) a DMF solution (6 mL) of HL (42.0 mg, 0.152 mmol) was added, affording a dark green solution. After stirring for 20 minutes, the dark green solution was filtered and diffusion of diisopropyl ether yielded dark green needles of  $[\text{Fe}(\text{L})_2(\text{H}_2\text{O})_2] \cdot 7\text{DMF}$  ( $\mathbf{5} \cdot 7\text{DMF}$ ). The crystals were collected by suction and air-dried. Anal. Calc. for  $[\text{Fe}(\text{L})_2(\text{H}_2\text{O})_2] \cdot 0.1\text{DMF}$ : C, 59.90; H, 3.22; N, 13.19 %. Found: C, 60.03; H, 3.50; N, 13.27 %. Selected IR (KBr): 1670(m,  $\nu_{\text{C=O}}$ ), 1647(s), 1470(m), 1223(s), 708(s)  $\text{cm}^{-1}$ .

### Synthesis of $[\text{Fe}(\text{HL})_3](\text{BF}_4)_2$ (6)

To an acetonitrile solution (2 mL) of  $\text{Fe}(\text{BF}_4)_2 \cdot 6\text{H}_2\text{O}$  (17.6 mg, 0.050 mmol) an acetonitrile solution (6 mL) of HL (41.2 mg, 0.15 mmol) was added, affording a reddish brown solution. After stirring for 10 minutes, the resulting clear solution was filtered and diffusion of diisopropyl ether in the fridge yielded dark red columnar crystals of  $[\text{Fe}(\text{HL})_3](\text{BF}_4)_2 \cdot 6\text{H}_2\text{O}$  ( $\mathbf{6} \cdot 6\text{H}_2\text{O}$ ). The crystals were collected by suction and air-dried. Anal. Calc. for  $[\text{Fe}(\text{HL})_3](\text{BF}_4)_2 \cdot 6\text{H}_2\text{O}$ : C, 49.56; H, 3.38; N, 10.84 %. Found: C, 49.48; H, 3.49; N, 11.03 %. Selected IR (KBr): 1672(s,  $\nu_{\text{C=O}}$ ), 1587(m), 1448(m), 1217(s), 1084(s,  $\text{BF}_4$ ), 793(m), 700(s)  $\text{cm}^{-1}$ .

### X-ray structure determinations

All data collections were performed on a Bruker SMART APEX II with a CCD area detector with graphite monochromated  $\text{Mo-K}\alpha$  ( $\lambda = 0.71073 \text{ \AA}$ ) radiation. All structures were solved by direct methods and refined by full-matrix least-squares methods based on  $F^2$  using the SHELXL software. Non-hydrogen atoms were refined anisotropically. All hydrogen atoms were positioned geometrically and refined with

isotropic displacement parameters according to the riding model. All geometrical calculations were performed using the SHELXL software. SQUEEZE treatments were applied for refinements of complexes **5** and **6** owing to the extreme disordering of the solvent molecules. Crystal data of all complexes are given in Tables S1 and S2 in the ESI.

#### Physical measurements

Infrared (IR) spectra were recorded (400–4000  $\text{cm}^{-1}$  region) on a SHIMADZU IRAffinity-1 spectrometer using KBr pellets. Direct current magnetic susceptibility measurements of polycrystalline samples were measured in the temperature range of 1.8–300 K with a Quantum Design MPMS-5XL SQUID magnetometer under an applied magnetic field of 500 Oe or 1 T. Data were corrected for the diamagnetic contribution calculated from Pascal's constants including the contribution of the sample holder.

Variable-temperature Mössbauer experiments were carried out using a  $^{57}\text{Co}/\text{Rh}$  source in a constant acceleration transmission spectrometer (Topologic Systems) equipped with an Iwatani HE05/CW404 Cryostat. The spectra were recorded in the temperature range of 20–300 K. The spectrometer was calibrated using standard  $\alpha\text{-Fe}$  foil.

## Results and discussion

### Synthesis and characterization

The heteroleptic complexes **1–4** with two kinds of bidentate ligands were synthesized following similar synthetic procedures. Using triethylamine as a base, the deprotonated anionic bidentate ligand  $\text{L}^-$  is expected to coordinate to an iron ion. Four complexes with two  $\text{L}^-$  and one neutral bidentate ligand ( $\text{L}^{1-4}$ ) were synthesized. Ligands  $\text{L}^1$  and  $\text{L}^2$  are common diamine molecules, forming very stable five-membered chelate rings upon complexation. On the other hand,  $\text{L}^3$  and  $\text{L}^4$  are known as non-innocent ligands, which can be converted to different electronic states with different molecular structures after deprotonation and oxidation (Scheme 1).<sup>12–13</sup> In this research, bidentate ligands  $\text{L}^{3a}$  and  $\text{L}^{4a}$ , the reduced forms of  $\text{L}^3$  and  $\text{L}^4$  respectively, were used during complexation reactions under atmospheric conditions, yielding mononuclear iron complexes with the oxidized forms of the ligands,  $\text{L}^{3c}$  and  $\text{L}^{4c}$ .

#### Crystal structure of **1**

**1** crystallized in the triclinic space group  $P\bar{1}$ . Single crystal X-ray analysis reveals that **1** consists of two deprotonated naphthoquinone ligands  $\text{L}^-$ , ethylenediamine  $\text{L}^1$ , one iron(II) ion, and lattice solvents (one DMF and two 1,4-dioxane) shown in Figure 1a. Both ligands coordinate to the iron ion in a bidentate fashion. The iron ion has an octahedral coordination geometry with six nitrogen donors. Hydrogen bonds link the imidazole moiety of  $\text{L}^-$  and ethylenediamine (Figure S1). Considering the coordination bond lengths, BVS calculations, and charge balance, the iron ion can be assumed to be divalent. At 100 K, the average coordination bond length is 2.003 Å, and  $\Sigma$  value is 49.87° consistent with an iron ion in the low spin state. At 270 K, the average bond length and  $\Sigma$  value<sup>12</sup> are

2.184 Å and 80.98°, respectively, consistent with iron(II) in the high spin state and confirming the onset of thermal SCO.

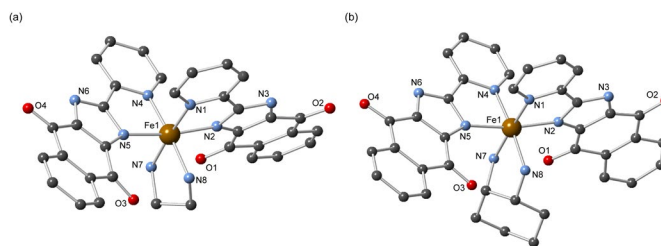


Fig. 1. Molecular structures of (a) **1** and (b) **2** at 100 K. Lattice solvents have been omitted for clarity. Colour code: C, gray; N, light blue; Fe(II), brown.

#### Crystal structure of **2**

**2** crystallized in the triclinic space group  $P\bar{1}$ . The structure of **2** is similar to that of **1** shown in Figure 1b. **2** consists of two  $\text{L}^-$ , *cis*-1,2-cyclohexanediamine, one iron(II) ion and lattice solvent of one DMF molecule. At 100 K, the average coordination bond length is 2.007 Å, and the  $\Sigma$  value is 50.00°. In contrast, the average bond length and  $\Sigma$  value are 2.179 Å and 79.70° at 270 K, respectively, indicative of thermal SCO. For **2**, there are hydrogen bonded interactions between the imidazole moiety of  $\text{L}^-$  and *cis*-1,2-cyclohexanediamine similar to those in **1** (Figure S2). Considering the molecular structures of **1** and **2**, the bidentate coordination site for ethylenediamine ( $\text{L}^1$ ) or *cis*-1,2-cyclohexanediamine ( $\text{L}^2$ ) will have a certain level of flexibility.

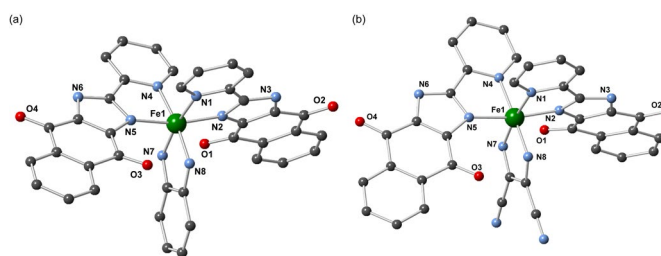
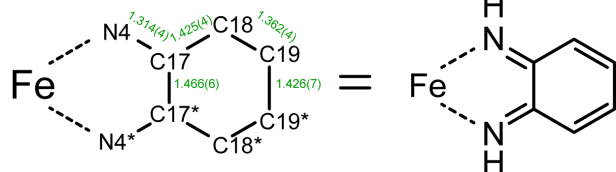


Fig. 2. Molecular structures of (a) **3** and (b) **4** at 100 K. Lattice solvents have been omitted for clarity. Colour code: C, gray; N, light blue; Fe(II), green.

#### Crystal structure of **3**

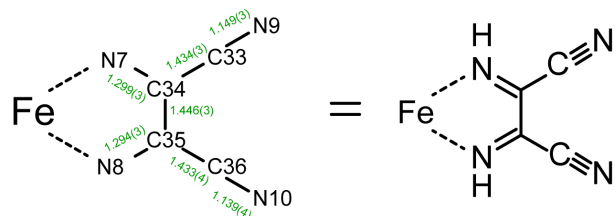
Complex **3** crystallized in the orthorhombic space group  $Fdd2$ . **3** consists of two  $\text{L}^-$ , one diiminobenzoquinone ( $\text{L}^{3c}$ ) and two DMF molecules as lattice solvent (Figure 2a). The complex has an inversion center at the centre of the complex on the iron ion. The assignment of the bidentate ligand  $\text{L}^{3c}$  was based on bond lengths (Scheme 2).<sup>13</sup> The average C17–N4 bond length of  $\text{L}^{3c}$  is 1.314 Å, indicating double bond character. In addition, C17–C18 and C17–C17\* bond lengths are consistent with single bonds. Therefore,  $\text{L}^{3c}$  can be assigned to the doubly deprotonated and two-electron oxidized state of  $\text{L}^3$ . As for the iron ion, the average coordination bond length of 1.964 Å, BVS calculations, charge balance, and the  $\Sigma$  value of 60.01° reveal that iron ion is in a divalent low spin state.



Scheme 2. Assignment of  $L^3$ . Schematic representation of bond length and chemical structure of  $Fe-L^3$  moiety.

#### Crystal structure of 4

**4** crystallized in the triclinic space group  $P\bar{1}$ . **4** has a similar structure to **3**, but the symmetry is lower. **4** consists of two  $L^1$ , one diiminosuccinonitrile ( $L^{4c}$ ) and two DMF molecules as lattice solvent (Figure 2b). The non-innocent ligand  $L^{4a}$  was also oxidized to  $L^{4c}$  as in compound **3**. This assignment was based on average bond length, 1.297 Å, of C34(C35)-N7(N8) of  $L^{4c}$  (Scheme 3).<sup>14</sup> The iron ion is divalent and low-spin, as confirmed by its average bond length of 1.949 Å, BVS calculations, charge balance, and the  $\Sigma$  value of 55.71°.



Scheme 3. Assignment of  $L^4$ . Schematic representation of bond length and chemical structure of  $Fe-L^4$  moiety.

#### Crystal structure of 5

Complex **5** crystallized in the triclinic space group  $P\bar{1}$ . **5** consists of two  $L^1$ , two water molecules, and seven DMF molecules in the crystal lattice (Figure 3a). There are two mononuclear  $[Fe(L)_2(H_2O)_2]$  molecules in one unit cell. Iron ions in both molecules are in the divalent high spin electronic states, as confirmed by an average coordination bond length of 2.155 Å, and a  $\Sigma$  value of 63.57°. Coordinated water molecules form hydrogen bonded interactions with the ligand oxygen atoms, with O5...O3 (O11...O7) and O6...O1 (O12...O9) distances of 2.710 (2.689) and 2.717 (2.689) Å, respectively.

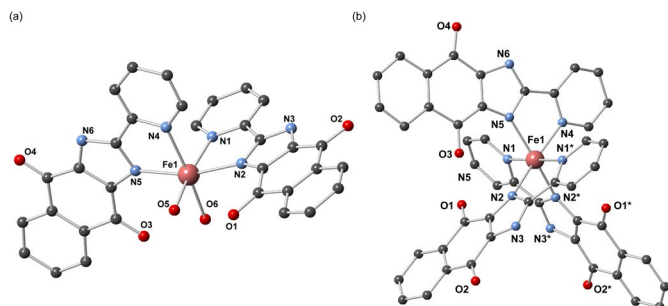


Fig. 3. Molecular structures of (a) **5** and (b) **6** at 100 K. Lattice solvents have been omitted for clarity. Colour code: C, gray; N, light blue; Fe(II), magenta. (symmetry code: \*,  $-x+1, +y, -z+1/2$ ).

#### Crystal structure of 6

Complex **6**, the homoleptic analogue, crystallized in the monoclinic space group  $C2/c$ . **6** consists of three protonated HL, two  $BF_4^-$  anions and twelve water molecules. The tris-chelate complex  $[Fe(HL)_3]^{2+}$  molecule has a two-fold rotation axis passing through the Fe ion and dissecting the N2 – N2\* vectors (symmetry code: \*,  $-x+1, +y, -z+1/2$ ).

#### Magnetic properties

Magnetic susceptibilities of all complexes were measured on polycrystalline samples. Temperature dependent magnetic susceptibilities are shown in Figure 4. Complexes **1** and **2** show similar SCO behavior. On the other hand, complexes **3** and **4** are diamagnetic, and complexes **5** and **6** are paramagnetic without remarkable change in  $\chi_m T$  values, suggesting no SCO. In **1** and **2**, the  $\chi_m T$  value at 300 K is 3.21 and 3.29  $\text{emu mol}^{-1} \text{K}$ , respectively. On cooling, the values of  $\chi_m T$  drop gradually around  $T_{1/2} = 218$  and 204 K, respectively, which are determined by a plot of the first derivative of  $\chi_m T$  vs.  $T$  (Figure S3). The spin transitions are almost complete at 100 K. The  $\chi_m T$  values at 100 K are 0.06 and 0.07  $\text{emu mol}^{-1} \text{K}$ , respectively. These SCO properties were confirmed by single crystal X-ray analyses and Mössbauer studies (*vide infra*). Thermodynamic parameters of the spin transition were obtained using the regular solution model of Schlichter and Drickamer,<sup>15</sup> which leads to the following equation for the high spin (HS) molecular fraction,  $\gamma_{HS}$ :

$$\ln[1-\gamma_{HS}]/\gamma_{HS} = [\Delta H + I(1-2\gamma_{HS})]/RT - \Delta S/R$$

where  $\Delta H$  and  $\Delta S$  are the enthalpy and entropy changes associated with spin transition, and  $I$  is the interaction parameter characterizing cooperativity. Figure S4 illustrates the simulated spin-crossover behaviour with parameters of  $\Delta H = 11.7 \text{ kJ mol}^{-1}$ ,  $\Delta S = 52.9 \text{ J mol}^{-1} \text{K}^{-1}$ , and  $I = 1.82 \text{ kJ mol}^{-1}$  for **1**,  $\Delta H = 13.1 \text{ kJ mol}^{-1}$ ,  $\Delta S = 65.0 \text{ J mol}^{-1} \text{K}^{-1}$ , and  $I = 0.26 \text{ kJ mol}^{-1}$  for **2**. The calculated thermodynamic parameters are close to those typically observed for mononuclear iron(II) SCO complexes.<sup>16</sup>

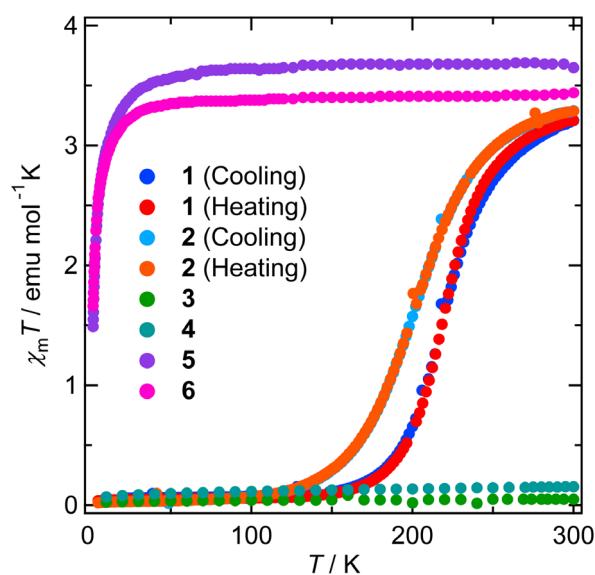


Fig. 4. Temperature-dependent magnetic susceptibility data for all complexes.

Complexes **3** and **4** are predominantly low spin. The  $\chi_m T$  values at 300 K for **3** and **4** are 0.05 and 0.15 emu mol<sup>-1</sup> K, respectively. These values are close to the expected spin only value for a diamagnetic low spin iron(II) ion. The  $\chi_m T$  values are almost constant from 300 K to 30 K. In the low temperature region the  $\chi_m T$  values for **3** and **4** decreased to 0.03 and 0.07 emu mol<sup>-1</sup> K at 10 K, respectively.

In the case of complexes **5** and **6**,  $\chi_m T$  values at 300 K for **5** and **6** are 3.65 and 3.44 emu mol<sup>-1</sup> K, respectively. The values are almost constant between 300 K and 50 K, and are close to the theoretical value expected for a high spin iron(II) ion ( $S = 2$ ). Below 50 K, these  $\chi_m T$  values abruptly decreased with decreasing temperature. At 1.8 K,  $\chi_m T$  values of **5** and **6** are 1.49 and 1.66 emu mol<sup>-1</sup> K, respectively. This decrease will be derived from intermolecular antiferromagnetic interactions and zero field splitting effects.

Considering ligand field strength of L<sup>1</sup>, L<sup>2</sup> and water molecule, the magnitude can be described as H<sub>2</sub>O < L<sup>2</sup> < L<sup>1</sup>.<sup>17</sup> In keeping with this trend, complex **5** with two water molecules is in the high spin state, and complexes **1** and **2** show spin crossover behavior. The transition temperature of **1** and **2** seem to change according to this order. This fact suggest that appropriate selection of a secondary ligand can effectively tune the SCO transition temperature.

#### Mössbauer spectra

The electronic states of the iron ions for all complexes were confirmed by Mössbauer spectroscopic analyses. For **1** and **2**, distinct changes in their spectra between 20 K and 300 K were observed, indicative of spin crossover behavior (Figures S5 and S6). In the case of complexes **3-6**, spectra were collected at 20 K (Figures S7 and S8). Considering the fitting parameters for the observed doublet peaks, it is concluded that the iron ions of **3** and **4** were in the low spin state and those of **5** and **6** were in high spin state (Table S3). Note that slightly large quadrupole splitting parameters for **3** and **4** may arise from the asymmetric coordination geometry of two L- ligand and the oxidized L<sup>3</sup> and L<sup>4</sup> ligands and the different electron donation characters of different ligands.

#### Conclusions

Here we have described the synthesis, structures and magnetic properties of a family of new heteroleptic iron complexes with a naphthoquinone-type ligand, 2-(pyridin-2-yl)-1H-naphtho[2,3-d]imidazole-4,9-dione (HL). Two spin-crossover complexes **1** and **2** were structurally characterized at 100 K and 270 K, and their gradual spin-crossover behaviors were observed by magnetic susceptibility measurements. Complexes **3** and **4**, bearing non-innocent ligands, were found to remain in the low spin state in the range of 2-300 K. The analogous aqua complex **5** and the homoleptic trischelate complex **6** were found to exist in the high spin state due to their weak ligand fields. These spin states were confirmed by

Mössbauer spectroscopy. The variation of spin state of these heteroleptic complexes with naphthoquinone ligands can be treated as a new class of useful spin crossover complexes, which can be finely tuned by the exchange of secondary ligands. The next generation of functional spin-crossover-active materials will depend on the fine-tuning of the phenomenon as presented here, and possibly the coupling of secondary tuneable 'tags', such as redox-active antenna that modify electronic structure, and Brønsted moieties that facilitate proton-driven dynamic molecular switching.

#### Conflicts of interest

There are no conflicts to declare.

#### Acknowledgements

This work was supported by a Grant-in-Aid for Scientific Research (C) (No. 17K05800), a Grant-in-Aid for Challenging Exploratory Research (No. 18K19088), and Grant-in-Aid for Scientific Research on Innovative Areas 'Coordination Asymmetry' (no. JP16H06523) from the Japan Society for the Promotion of Science (JSPS).

#### Notes and references

- 1 L. Spiccia, G.B. Deacon, C.M. Kepert, *Coord. Chem. Rev.*, 2004, **248**, 1329; A.K. Pal, G.S. Hanan, *Chem. Soc. Rev.*, 2014, **43**, 6184; Y. Zhang, M. Schlz, M. Wächtler, M. Karnahl, B. Dietzek, *Coord. Chem. Rev.*, 2018, **356**, 127.
- 2 S. Fukuzumi, *Phys. Chem. Chem. Phys.*, 2008, **10**, 2283; Y. Pellegrin, F. Odobel, *Coord. Chem. Rev.*, 2011, **255**, 2578; L. Hammarström, *Acc. Chem. Res.*, 2015, **48**, 840.
- 3 P. Gütllich and H.A. Goodwin Eds. *Spin Crossover in Transition Metal Compounds I, II, and III*, Springer-Verlag, Berlin, Germany, 2004; A. Bousseksou, G. Molnár, L. Salmon and W. Nicolazzi, *Chem. Soc. Rev.*, 2011, **40**, 3313-3335; M.A. Halcrow, *Chem. Soc. Rev.*, 2011, **40**, 4119-4142; J. Olguín and S. Brooker, *Coord. Chem. Rev.*, 2011, **255**, 203-240; P. Gütllich, Y. Garcia and H.A. Goodwin, *Chem. Soc. Rev.*, 2000, **29**, 419-427; D.J. Harding, P. Harding and W. Phonsri, *Coord. Chem. Rev.*, 2016, **313**, 38-61; P. Guionneau, *Dalton Trans.*, 2014, **43**, 382-393; P. Gamez, J.S. Costa, M. Quesada and G. Aromí, *Dalton Trans.*, 2009, **38**, 7845-7853.
- 4 M. Wicholas, R.S. Drago, *J. Am. Chem. Soc.*, 1968, **90**, 6946; T. Saji, T. Fukai, S. Aoyagui, *J. Electroanal. Chem.*, 1975, **66**, 81; T. Fujiwara, K. Matsuda, Y. Yamamoto, *Inorg. Nucl. Chem. Lett.*, 1980, **16**, 301; T. Fujiwara, E. Iwamoto, Y. Yamamoto, *Inorg. Chem.*, 1984, **23**, 115; S. Musumeci, E. Rizzarelli, I. Fragalà, S. Sammartano, R.P. Bonomo, *Inorg. Chim. Acta*, 1973, **7**, 660; G.A. Renovitch, W.A. Baker, *J. Am. Chem. Soc.*, 1968, **90**, 13; A.M.A. Bennett, G.A. Foulds, D.A. Thornton, G.M. Watkins, *Spectrochim. Acta*, 1990, **46A**, 13.
- 5 M. Sorai, J. Ensling, P. Gütllich, *Chem. Phys.*, 1976, **18**, 199; E. Konig, *Prog. Inorg. Chem.*, 1987, **35**, 527; T. Nakamoto, A. Bhattacharjee, M. Sorai, *Bull. Chem. Soc. Jpn.*, 2004, **77**, 921; S. De, L.-M. Chamoreau, H.E.I. Said, Y. Li, A. Flambard, M.-L. Boillot, S. Tewary, G. Rajaraman, R. Lescouëzec, *Front. Chem.*, 2018, **6**, 326; J.R. Sams, T.B. Tsin, *J. Chem. Soc., Dalton Trans.*, 1976, 488; A.W. Addison, S. Burman, C.G. Wahlgren, *J. Chem. Soc., Dalton Trans.*, 1987, 2621; J.R. Sams, J.C. Scott, T.B. Tsin, *Chem. Phys. Lett.*, 1973, **18**, 451; J.R. Sams, T.B. Tsin, *Inorg.*

- Chem.*, 1976, **15**, 1544; A.T. Baker, H.A. Goodwin, *Aust. J. Chem.*, 1977, **30**, 771; R. Boča, P. Baran, L. Dlháň, J. Šima, G. Wiesinger, F. Renz, U. El-Ayaan, W. Linert, *Polyhedron*, 1997, **16**, 47; J.J. Hrudka, H. Phan, J. Lengyel, A.Y. Rogachev, M. Shatruk, *Inorg. Chem.*, 2018, **57**, 5183; N. Bibi, E.G.R. de Arruda, A. Domingo, A.A. Oliveira, C. Galuppo, Q.M. Phung, N.M. Orra, F. Beron, A. Paesano, K. Pierloot, A.L.B. Formiga, *Inorg. Chem.*, 2018, **57**, 14603; H.S. Scott, R.W. Staniland, P.E. Kruger, *Coord. Chem. Rev.*, 2018, **362**, 24.
- 6 H. Phan, J.J. Hrudka, D. Igimbayeva, L.M.L. Daku and M. Shatruk, *J. Am. Chem. Soc.*, 2017, **139**, 6437.
- 7 J.A. Real, M.C. Muñoz, J. Faus, X. Solans, *Inorg. Chem.*, 1997, **36**, 3008; N. Moliner, L. Salmon, L. Capes, M.C. Muñoz, J.-F. Létard, A. Bousseksou, J.-P. Tuchagues, J.J. McGarvey, A.C. Dennis, M. Castro, R. Burriel, J.A. Real, *J. Phys. Chem. B*, 2002, **106**, 4276-4283; A.L. Thompson, A.E. Goeta, J.A. Real, A. Galet, M.C. Muñoz, *Chem. Commun.*, 2004, 1390; H. Naggert, A. Bannwarth, S. Chemnitz, T. von Hofe, E. Quandt, E. Tuzcek, *Dalton Trans.*, 2011, **40**, 6364; X. Zhang, T. Palamarciuc, J.-F. Létard, P. Rosa, E.V. Lozada, F. Torres, L.G. Rosa, B. Doudin, P.A. Dowben, *Chem. Commun.*, 2014, **50**, 2255; E. Ludwig, H. nagger, M. Kalläne, S. Rolhf, E. Kröger, A. Bannwarth, A. Quer, K. Rossnagel, L. Kipp, and F. Tuzcek, *Angew. Chem. Int. Ed.*, 2014, **53**, 3019.
- 8 Y.-H. Luo, M. Nihei, G.-J. Wen, B.-W. Sun, H. Oshio, *Inorg. Chem.*, 2016, **55**, 8147; J. Ru, F. Yu, P.-P. Shi, C.-Q. Jiao, C.-H. Li, R.-G. Xiong, T. Liu, M. Kurmoo, J.-L. Zuo, *Eur. J. Inorg. Chem.*, 2017, 3144; S. Xue, Y. Guo, A. Rotaru, H. Müller-Bunz, G. G. Morgan, E. Trzop, E. Collet, J. Oláh, Y. Garcia, *Inorg. Chem.*, 2018, **57**, 9880.
- 9 E. E. König, K. Madeja, K.J. Watson, *J. Am. Chem. Soc.*, 1968, **90**, 1146; K. Madeja, E. König, *J. Inorg. Nucl. Chem.*, 1963, **25**, 377; M. Golding, K.F. Mok, J.F. Ducan, *Inorg. Chem.*, 1966, **5**, 744; K. König, K. Madeja, *Inorg. Chem.*, 1967, **6**, 48; P. Ganfulim, P. Gütlich, E.W. Müller, W. Irlner, *J. Chem. Soc., Dalton Trans.*, 1981, 441; B. Gallois, J.-A. Real, C. Hauw, J. Zarembowitch, *Inorg. Chem.*, 1990, **29**, 1152; K. Akabori, H. Matsuo, Y. Yamamoto, *J. Inorg. Nucl. Chem.*, 1973, **35**, 2679; E.W. Müller, H. Spiering, P. Gütlich, *Chem. Phys. Lett.*, 1982, **93**, 567; M. Reiher, *Inorg. Chem.*, 2002, **41**, 6928.
- 10 T. Shiga, E. Oshiro, N. Nakayama, K. Mitsumoto, G.N. Newton, H. Nishikawa, H. Oshio, *Eur. J. Inorg. Chem.*, 2013, **2013**, 577; T. Matsumoto, G.N. Newton, T. Shiga, S. Hayami, Y. Matsui, H. Okamoto, R. Kumai, Y. Murakami, H. Oshio, *Nat. Commun.*, 2014, **5**, 3865; T. Shiga, Y. Sato, M. Tachibana, H. Sato, T. Matsumoto, H. Sagayama, R. Kumai, Y. Murakami, G.N. Newton, H. Oshio, *Inorg. Chem.*, 2018, **57**, 14013; T. Shiga, R. Saiki, L. Akiyama, R. Kumai, D. Natke, F. Renz, J. Cameron, G.N. Newton, H. Oshio, *Angew. Chem. Int. Ed.*, 2019, **58**, 5658; R. Saiki, H. Miyamoto, H. Sagayama, R. Kumai, G.N. Newton, T. Shiga, H. Oshio, *Dalton Trans.*, 2019, **48**, 3231.
- 11 R. Manivannan, A. Satheshkumar, K.P. Elango, *New J. Chem.*, 2013, **37**, 3152; C. Parthiban, S. Ciattini, L. Chalazzi, K.P. Elango, *Sens. Actuator B Chem.*, 2016, **231**, 768; L. Pan, Q. Zheng, Y. Chen, R. Yang, Y. Yang, Z. Li, X. Meng, *Eur. J. Med. Chem.*, 2018, **157**, 423; Z. Liu, Z. Zhang, W. Zhang, D. Yan, *Bioorg. Med. Chem. Lett.*, 2018, **28**, 2454.
- 12 P. Guionneau, C. Brigouleix, Y. Barrans, A.E. Goeta, J.-F. Létard, J.A. Howard, J. Gaultier, D.C. Chasseau, *C. R. Acad. Sci., Ser. IIc* 4, 2001, 161; P. Guionneau, M. Marchivie, G. Bravic, J.F. Létard, D Chasseau, *Top. Curr. Chem.* 2004, **234**, 97.
- 13 S.-M. Peng, C.-T. Chen, D.-S. Liaw, C.-I. Chen, Y. Wang, *Inorg. Chim. Acta*, 1985, **101**, L31; G. Christoph, V. L. Goedken, *J. Am. Chem. Soc.*, 1973, **95**, 3869; M.M. Bittner, S.V. Lindeman, C.V. Popescu, A.T. Fiedler, *Inorg. Chem.*, 2014, **53**, 4047; T. Matsumoto, H.-C. Chang, M. Wakizaka, S. Ueno, A. Kobayashi, A. Nakayama, T. Taketsugu, M. Kato, *J. Am. Chem. Soc.*, 2013, **135**, 8646.
- 14 C.-T. Chen, D.-S. Liaw, G.-H. Lee, S.-M. Peng, *Transition Met. Chem.*, 1989, **14**, 76.
- 15 C. P. Slichter, H.G. Drickamer, *J. Chem. Phys.*, 1972, **56**, 2142.
- 16 L. Capes, J.-F. Létard, O. Kahn, *Chem. Eur. J.*, 2000, **6**, 2246; C. Genre, E. Jeanneau, A. Bousseksou, D. Luneau, S.A. Borshch, G.S. Matouzenko, *Chem. Eur. J.*, 2008, **14**, 697; T. Romero-Morcillo, F.J. Valverde-Muñoz, L. Piñeiro-López, M.C. Muñoz, T. Romero, P. Molina, J.A. Real, *Dalton Trans.*, 2015, **44**, 18911.
- 17 M. Brorson, M.R. Dyxenburg, F. Galsbøl, K. Simonsen, *Acta Chem. Scand.*, 1996, **50**, 289.